Research Journal of Applied Sciences, Engineering and Technology 3(12): 1421-1429, 2011
ISSN: 2040-7467

Submitted: July 26, 2011 Accepted: September 18, 2011 Published: December 26, 2011

Investigating Different ZnO Arresters Models against Transient Waves

A. Babaee, R. Ebrahimi, M. Hoseynpoor and M. Najafi
Department of Engineering, Bushehr Branch, Islamic Azad University, Bushehr, Iran

Abstract: Metal oxide surge arresters have dynamic characteristics that are significant for over voltage coordination studies involving fast front surges. Several models with acceptable accuracy have been proposed to simulate this frequency-dependent behavior. In this paper, various electrical models are presented for surge arrester performance simulation against lightning impulse. The desirable model is obtained by using simulation results of the existing models and experimental tests. The IEEE proposed model is a proportional model can give satisfactory results for discharge currents within a range of time to crest for 0.5 to 45 μs but due to no existing residual voltage resulting switching current on the manufacture's datasheets decrease its performance generally. In this study the maximum residual voltage due to current impulse is analyzed too. In additional, the amount of discharged energy by surge arrester is focused.

Key words: Current impulse wave,dynamic characteristics, residual voltage, ZnO arresters

INTRODUCTION

In recent years, using metal oxide (ZnO) arresters is a common and prevalent affair for transformers, capacitance banks etc protection against impulse over voltages. Therefore, correct and accurate investigation of ZnO arresters behavior in power networks requires correct simulation in the existing transient state software. Several papers have been presented under arresters modeling title (Gupta, 1990; Ahmad, 1994; Daniel, 1985; Ravinda and Singh, 2002; Diaz *et al*., 2001) each has concerned different parameters in simulation process.

At the beginning, the arrester was just modeled by a nonlinear resistance due to the nonlinear feature of the varistor tablets. The leakage capacitances stand around the arrester were then under consider in transient state simulations due to high frequency bands (spectrums) existence. This was specially confirmed according to the crystal shaped structure of varistors. In investigations accomplished between the waveforms resulted by voltage residual and the arresters discharge current, a series inductance was added to the arrester model due to a short delay exists in current peak and the voltage peak waveforms. Some other models were reported by Daniel (1985) and then with IEEE workgroup (1992) because the mentioned inductance was just properly performing in a limited range of frequencies. The IEEE model was an appropriate model from quality and quantity view point but was sensibly loosing its efficiency and was creating difficulties in modeling process due not existence of voltage switching information in majority of catalogs (according to difficulty of such test). Therefore, other models were presented to overcome such problem inspired by this model (Kim *at el*., 1996; Pinceti and Giannettoni, 1999).

In this study, the residual voltage of the arrester of qualitative and quantitative aspects is under consider as well as the discharged energy value, unlike other papers just have investigated the maximum value of impulse caused residual voltage.

INVESTIGATING THE STRUCTURE AND GENERAL MODEL OF ARRESTER

In a power circuit, an arrester is in charge of the follows:

- Leakage Current for normal mode utilization voltages
- Discharge Current during the over voltages, and discharging the energy the transient wave (without short circuit fault creation) (Daniel, 2001)

In result, the arrester should have a high rated resistance during system's normal utilization, posses a very low resistance during transient over voltages, and have a completely nonlinear V-I characteristics.

The crystal shaped structure of ZnO along with other metal oxides confirms the fact that it is possible to present a model comprised of a nonlinear and a parallel capacitor that is shown in Fig. 1. The V-I characteristics of a ZnO arrester is approximately as Fig. 2. Two current types pass through nonlinear resistances according to the presented waveform. The leakage current with rating of 0.1-0.8 mA is created due to the existence of steady state 50 Hz voltage on arresters and a current called discharge current passes through the arrester due to lightning and switching caused voltage waveforms.

It is not necessary to consider temperature effects to show the transient over voltages type in simulation

Corresponding Author: A. Babaee, Department of Engineering, Bushehr Branch, Islamic Azad University, Bushehr, Iran

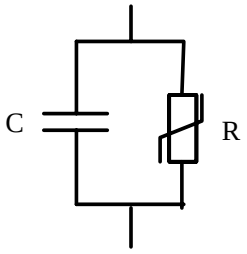

Fig. 1: The proposed model based on tablet material of metal oxide arrester

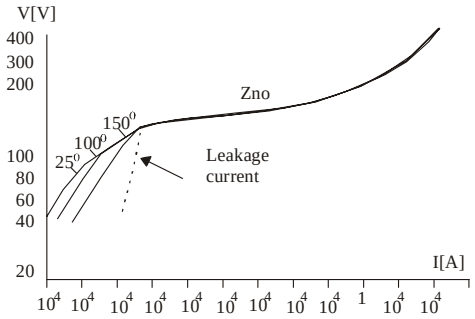

Fig. 2: The V-I characteristics of a ZnO arrester (static characteristics)

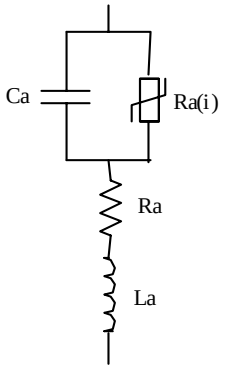

Fig. 3: The completed model presented by Popov (2002)

process since the arrester accepted current range in such investigations is more than 10mA. It is important to note that the thermal dependency is an important factor in selecting the arrester's operation domain under steady state and temporary over voltages conditions. Therefore, the temperature effect is neglected in modeling process. The effect of environment and the arrester box pollution are usually neglected.

More precision on the results of the simulation and the experimental data well clarify the fact that there exist a difference between the waveforms obtained from the experiments and the peak residual voltage values of the arresters. The differences can be notified as follows:

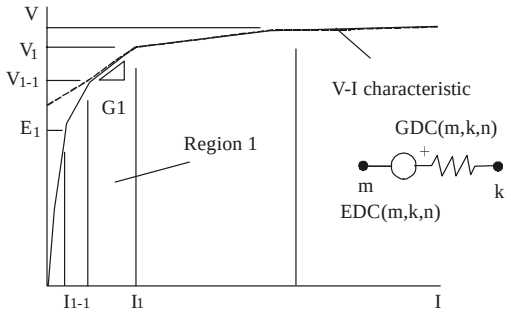

Fig. 4: linear estimation of arrester's V-I characteristic

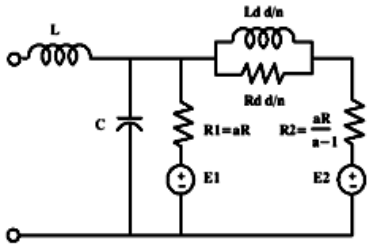

Fig. 5: The proposed ZnO arrester model for fast steep front waves

- The waves obtained by experiments posses more residual voltage peak values in impulse waves with fast steep front.
- The arresters' discharge current shows a considerable delay time compared with the residual voltage waves passing on arresters.

The mentioned reasons resulted in adding an inductor and a resistor where the inductor indicates the current to voltage delay time. Figure 3, shows this complete model that presented by Popov in (Popov *et al*., 2002). Here, the arrester faces with more residual voltage peak at the first moment in compare with the previous model, due to the existence of inductor and the resistor against the current flow. The V-I characteristics of the ZnO arrester is expressed in several forms such as $i = P(v/v_{ref})^q$ (Vref is the arbitrary reference voltage) or $i = kV\alpha$ or $U = ki^{1/\alpha}$. This characteristic is exponential exists in the data sheets delivered by the arrester manufacturer.

SOME OF PRESENTED MODELS FOR ARRESTER SIMULATION

In this section, some popular models of arresters are presented and investigated as below:

D. W. Durbak model: The arrester model is obtained upon V-I characteristic and shows a unique resistance and

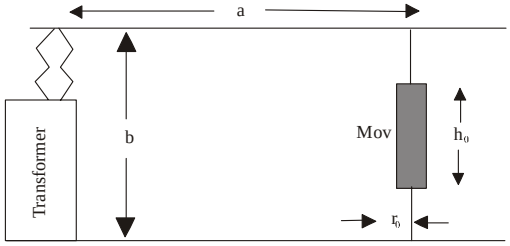

Fig. 6: The arrester loop circuit

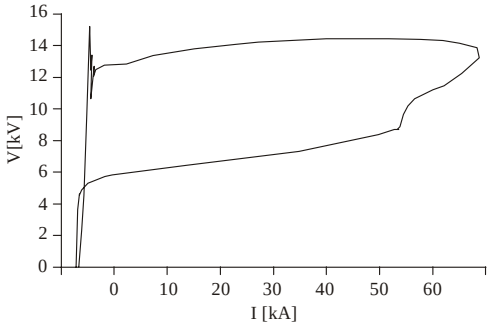

Fig. 7: The dynamic characteristics of a ZnO varistor

dc voltage as follows under each different V and I condition due to its nonlinear characteristic.

Based on Fig. 4, a model was presented to the IEEE impulse wave protective devices committee (W.G.3.4.11) by D. W. Durbak in 29th September 1983 in "arrester modeling techniques" meeting held in Memphis Tennessee as Fig. 5.Where:

L : loop inductance
C : the leakage capacitor
R : The equivalent arrester resistance
Ld : 10 μH/m
Rd : 20 Ω/m
d : Tablets column length
n : The number of columns
a = 16

In such circuit, the loop created between arrester and the protected device possesses L valued inductance. The inductance value of this loop can be obtained as follows:

$$L = 10^{-7}\left[2b\ln\left(\frac{a}{r_0}\right) + h_0\right] \quad (1)$$

Also the arrester loop circuit is shown in Fig. 6. If in some cases the loop inductance is not clearly mentioned, it can approximately considered as 1 μH/m. The arrester

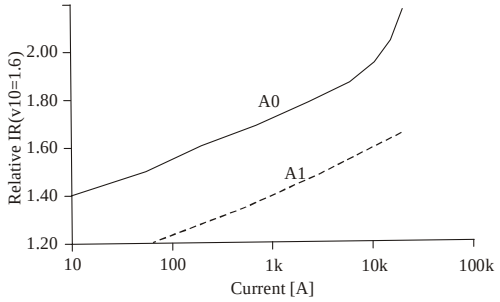

Fig. 8: The V-I characteristics of nonlinear resistance parts of the model

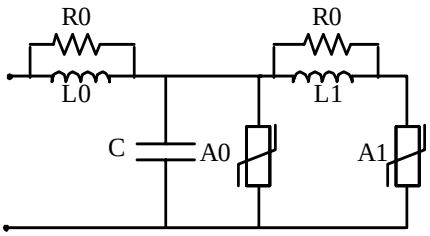

Fig. 9: The frequency model of metal oxide arrester

capacitor can be considered to stand in 600-4000 pF range.

IEEE workgroup model: IEEE workgroup 3.4.11 (1992) has reviewed a series of metal oxide arresters modeling methods for arrester modeling. The laboratory data of discharge voltage and accessible metal oxide arrester currents justified the group that the metal oxide arresters posses a mechanical characteristics valuable in lightning and other fast frontal waves investigation. This dynamic characteristic is shown in Fig. 7.

The model evaluated by IEEE workgroup was a frequency dependant model consists of two nonlinear A0 and A1 parts separated by a RL filter. The impedance of this filter is considerably low for the impulse waves with slow frontal, which makes two nonlinear parts to be considered as a parallel. The filter impedance is considered higher for fast frontal impulse waves in a way that the current flow through A0 is more than that of A1. Therefore, the A0 characteristic has a higher voltage level for a particular current, in compare with A1 (this can be observed in Fig. 8 and 9). According to Fig. 9, the presented model is completely synchronous with the behavior of a metal oxide arrester since it shows faster voltage discharge capability in compare with the faster frontal impulse waves. This model in its more progressive state can create more sections adding RL filters. However, just the two-part model was investigated by the IEEE workgroup because it was in good relation with laboratory data. This model shows very satisfying results for the waves with 0.5-4.5 μs frontal time.

For selecting frequency model parameters, we have:

d : the estimated arrester relation in meters
n : the number of tablets parallel column
L_1 : and R_1: the RL filter parameters
L_0 : the magnetic field inductance around the arrester
R_0 : to guaranty the calculation program convergence
C : the external capacitor installed between two arrester terminals

$$L_1 = 10d / n \quad R_1 = 65d / n$$
$$L_0 = 0.2d / n \quad R_0 = 100d / n \qquad (2)$$
$$c = 100n / d$$

Step 1: applying the above relations to obtain the primary values

Step 2: adapting the per unit values of A0 and A1 curves to achieve a proper adoption with the discharge voltages introduced by the manufacturer for current switching waves with more than 45 μs rising time.

Step 3: adapting L1 value to achieve the arrester discharge voltages adoption for 8.2 μs discharge currents accomplished through a iteration and averaging approach with error percentage acceptance.

A0 and A1 nonlinear resistances values presented in Fig. 9 are used to determine the primary values in a way that the discharge voltage value of each nonlinear resistance is obtained by follows:

$$\text{Discharge kV} = \text{IR} \times V_{10}/16 \qquad (3)$$

Pinceti and Giannetoni model: This model is achieved by simplifying the IEEE model and is presented in Fig. 10. The elements values are obtained through the following relations:

$$L_1 = \frac{1}{4} \cdot \frac{V_r 1/T_2 - V_r 8/20}{V_r 8/20} \cdot V_n \qquad (4)$$

$$L_0 = \frac{1}{12} \cdot \frac{V_r 1/T_2 - V_r 8/20}{V_r 8/20} \cdot V_n \qquad (5)$$

where
V_n : nominal arrester voltage
V_r 1/T2 : the residual voltage of 10 kA current impulse 1/T2 μs
V_r 8/20 : the residual voltage of 10 kA current impulse 8.20 μs,
R : is considered about 1 MΩ to avoid numerical calculation oscillations

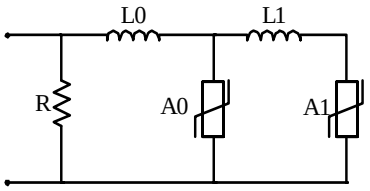

Fig. 10: the Pinceti and Giannetoni presented model

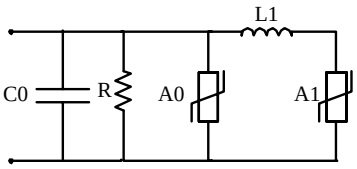

Fig. 11: Diaz-Fernandez suggested model

Two A0 and A1 nonlinear resistance characteristics definition is based on the curves shown in Fig. 8 (the curves are achieved through the IEEE workgroup suggested curves). In Li *et al*. (2002), these two models are presented in addition to IEEE frequency model, where a numerical optimization technique based approach is presented to determine the equivalent MOA (Metal Oxide Arrester) circuit. Parameters are detected based on the MOA residual voltage measured by 8/20 μs current pulse test measuring devices and MOA dimension information is not required despite the previous approach. This reference finally claims that applying the optimized IEEE suggested model through this numerical approach provides the most accuracy by investigating and evaluating the energy losses, primary angle factor of the residual voltage, peak residual voltage, and comparing the anticipated values by the measured ones.

Diaz-Fernandez suggested model: In (Diaz *et al*., 2001) Diaz and Fernandez presented a simplified IEEE model which faces with less than 4.5% residual peak voltage error for current waves with 1-30 μs frontal to overcome the problems exist in calculation and parameters regulation of IEEE frequency model such as iterative try and error processes and essential information lack. The proposed model is shown in Fig. 11. According to the suggested model, the parameters in Fig. 11, obtain by following stages:

Stage 1: A0 and A1 characteristic values are initially determined for lightning discharge currents using residual voltages (using $\gamma = 0.02$ for I0 in a way that I0 and I1 are the currents passing through A0 and A1 respectively which results in I0+I1 = I8/20). It is important to note that the $\gamma = 0.02$ assumption entails good accuracy (Fernandez, 2001).

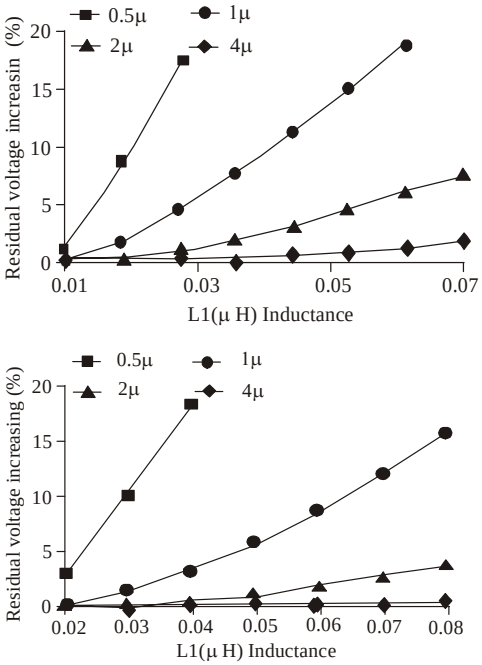

Fig. 12: The L1 related curve (a) for 50 kA block, (b) for 10 kA block

Stage 2: The residual voltage increase percentage for arrester nominal current is calculated through the followings:

$$\Delta V_{res}\ \% = \frac{U_{\ln,T_1} - U_{\ln,8/20}}{U_{\ln,8/20}} \times 100 \qquad (1)$$

where,

$U_{In,T1}$: residual voltage for discharge current with T1 suggested time and nominal amplitude

$U_{In,\ 8/20}$: residual voltage for lightening discharge current with nominal amplitude and 8.2 μs time interval

Stage 3: Roper L1 amount is selected using ΔVres%, T1 and two following curves (Fig. 12).

Stage 4: According to the fact that the above curves are obtained for 1 kV varistors, the L1 correct value is obtained using the following:

$$n = \frac{U_{in,8/20}\ \ for\ a\ complete\ arrester}{U_{in,8/20}\ \ for\ a\ 1KV\ block} \qquad (7)$$

The data of fraction of Eq. (7) is achieved by Table 1 which shows the residual peak voltage in 1 kV varistor.

Stage 5: The terminal capacitor, C0, is achieved as follows:

$$C_0 = \frac{100}{d}\ [\text{pF}] \qquad (8)$$

where d is total arrester height:

Stage 6: Finally, R is chosen as 1 MΩ for medium voltage arresters, and 10 MΩ for higher voltage levels. This resistance is chosen to avoid numerical calculations oscillations of computer program and is not significantly important.

SIMULATION RESULTS

A Toos arrester factory (In Iran) varistor is simulated in PSCAD (2003) and is qualitatively and quantitatively, compared with the actual wave form for the discharge test (accordingto IEEE C62.11 standard (1992)). The practical test circuit and the simulation in PSACD/EMTDC are well shown in Fig. 13 and 14. The overall characteristics of the considered varistor are as follows:

- Nominal current: 10kA
- Dimension: diameter×height (dmm×hmm): 50×30
- The residual voltage of 8.59/20.1 μs and10.04 kA is 11.47 kV
- The residual voltage of 4.31/10.5 μs and 9.97 kA is 12.14 kV
- The residual voltage of 250/2500 μs, 75A switching wave is 6.8 kV

The complete test circuit characteristics are as follows:

T : 220 V/80 V, 10 kVA, 50 Hz transformer
D : 200kV, 4 200mA rectifier bridge
R1, R2 : 200 MΩ and 20 kΩ dc voltage dividers
R01 : 12kΩ charge resistance
R02 : 10kΩ discharge resistance
K1 : discharging switch to ground
C : 122μF* pulse capacitor
R : 1, 1.5 and 2 Ω adoption resistances
L : adoption inductance consists of 10 coils

Table 1: The residual peak voltage in 1 KV varistor

Lightening discharge Current 8/20 [A]			Peak voltage [KV]	
I_1	I_0	I	10 KA block	5 KA block
1470	30	1500	2.73	2.87
2940	60	3000	2.90	3.07
4900	100	5000	3.07	3.07
9800	200	10000	3.60	3.33
19600	400	20000	3.70	74.27
39200	800	40000	4.53	5.30

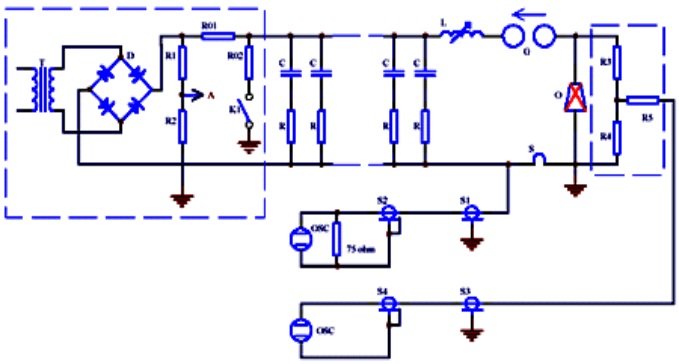

Fig. 13: Practical test circuit

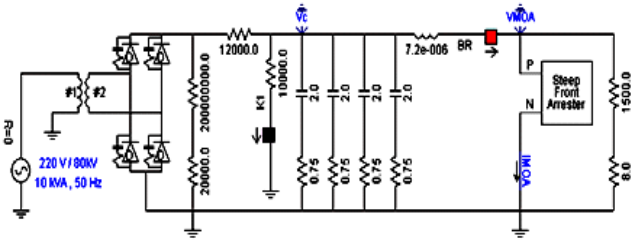

Fig. 14: Simulating the test circuit in PSCAD (2003)

G : the gap
O : under test device
S : 100 kA (1.4436 mΩ), (2.5838 Ω) measurement shunt resistance
R3, R4 : 1.5 and 8 Ω discharge voltage divider
S1, S2 and S3
: measuring cable(75Ω impedance)

OSC: TDS3012B type oscilloscope. The test and the simulation resulted waves are presented in Figs. 15 to 19. In test obtained curve, the current waveform time scale is two times more than that of the voltage waveform (2.5 μs/Div versus 5 μs/Div). In addition, the current waveform in the practical test is reversely plotted. In this paper, only the 8/20 μs current impulse caused waveforms are illustrated. The obtained waveforms are investigated from quality and quantity viewpoints through the following definitions.

Ip[kA] : peak impulse current
t[μs] Ur[kV]

: peak residual voltage
t1[μs] : voltage wave frontal time
t2[μs] : voltage wave rear time
Δ : Delay time of the current peak to the voltage peak
td[μs] : Voltage wave oscillations attenuation time
f[MHz]: Voltage wave oscillations frequency
e% : Error percentage of each parameter
w : density of error according to the importance of which for current and voltage peak values is considered as 1, and is assumed to be 0.001 for attenuation time and oscillations frequency, and equals to 0.1 for other parameters.
Er% : total error percentage calculated as follows as the same as the definition presented in (Penchenat, 1992):

$$Er\% = \sqrt{\frac{1}{N}\sum_{j=1}^{N}(w \times e_j)^2} \qquad (9)$$

Also, in continue, each model is investigated from discharged energy amount or on the other hand from the voltage and current under curve area point of view. The comparison and results obtained by discharged energy

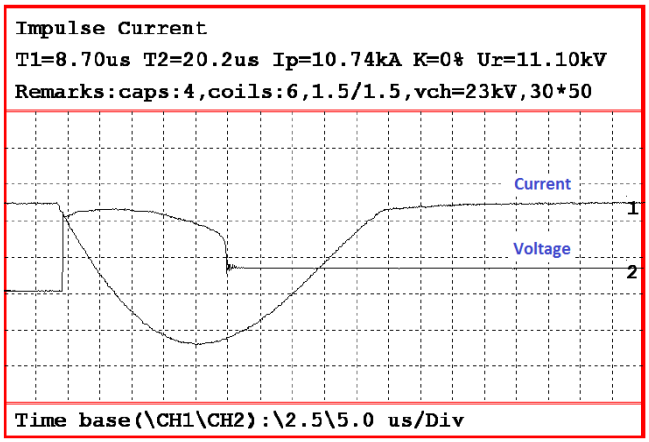

Fig. 15: Test resulted curves (reversed current)

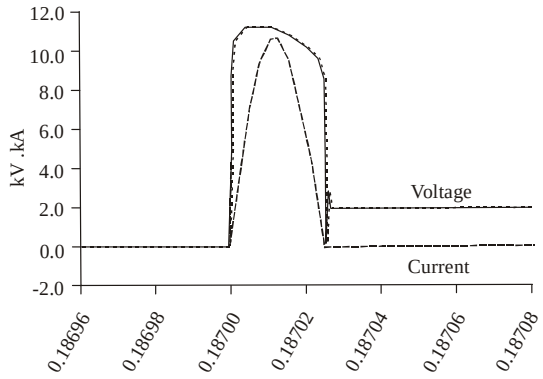

Fig. 16: Simulation resulted residual voltage of 8/20 µs current wave for IEEE model (Ip = 10.67 kA, Ur = 11.30kV)

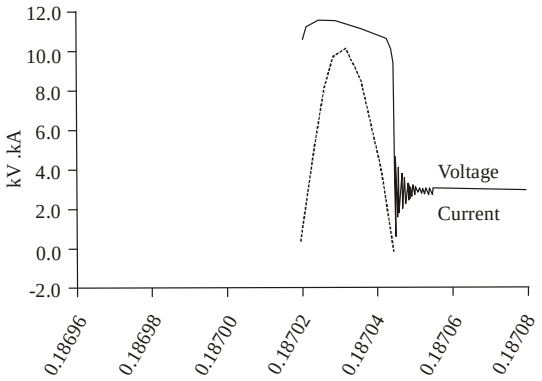

Fig. 18: Simulation resulted residual voltage of 8/20 µs current Durbak model (Ip = 10.32kA, Ur = 11.70kV)

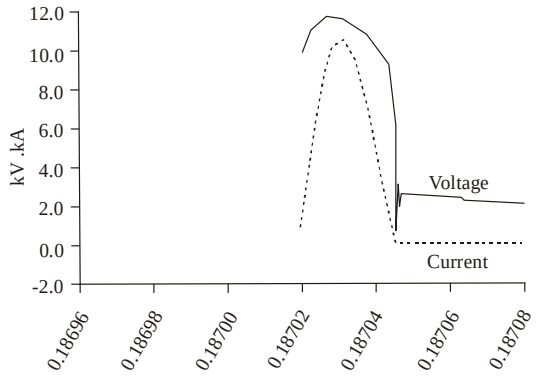

Fig. 17: Simulation resulted residual voltage of 8/20 µs current Diaz-Fernandez model (Ip = 10.47 kA, Ur = 11.63 kV)

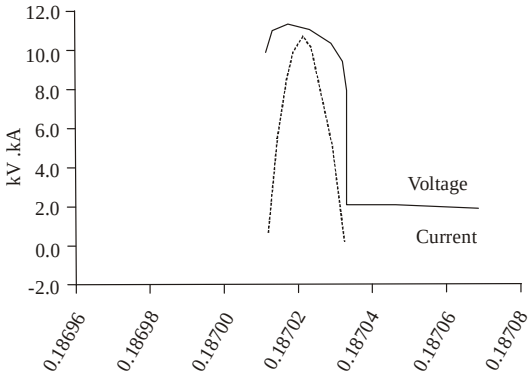

Fig. 19: Simulation resulted residual voltage of 8/20 µs current Pinceti model (Ip = 10.68 kA, Ur = 11.32 kV)

amount or on the other hand from the voltage and current under curve area point of view. The results are shown in Table 2 and 3.

The following experimental relation presented in (Penchenat, 1992) is applied to calculate the discharged energy amount since it is difficult to calculate the under curve area:

$$W = k \times V_{max} \times I_{max} \quad [Joules] \tag{10}$$

Table 2: Comparison of real result by simulated results for 8/20 μs wave

		Voltage						
Arrester model	I_p [kA]	U_r [kV]	t_1 [μs]	t_2 [μs]	Δ [μs]	t_d [μs]	f [MHz]	Er%
IEEE	10.69	11.30	7.50	25	3.50	2.50	0.80	
w× e%	- 0.46	1.80	- 1.18	0.2	1.67	- 1.01	- 0.07	1.05
Diaz	10.47	11.63	9.00	25	3.00	3.00	1.30	
w× e%	- 2.51	4.77	0.59	0.2	0.00	0.01	- 0.06	5.27
Durbak	10.32	11.70	6.00	25	6.00	12.00	2.00	
w× e%	- 3.91	5.40	- 2.94	0.2	10.00	0.34	- 0.04	4.68
Pinceti	10.68	11.32	6.50	25	4.00	0.00	0.00	
w×e%	- 0.56	1.98	- 2.35	0.2	3.33	- 0.10	- 0.11	1.73

Table 3: Comparison of real result by simulated results for 4/10 μs wave

		Voltage						
Arrester model	Ip[kA]	Ur [kV]	t1 [μs]	t2 [μs]	Δt [μs]	td [μs]	f [MHz]	Er%
IEEE	65.64	15.79	3.00	9.00	2.00	1.0	1.00	
w× e%	7.36	- 6.7	- 1.43	- 3.33	3.33	0.0	- 0.07	4.20
Diaz	64.47	18.7	1.50	9.00	4.00	0.0	0.00	
w× e%	5.45	1026	- 5.71	- 3.33	16.67	- 0.1	- 0.10	8.08
Durbak	65.4	17.22	1.50	10.00	3.50	0.0	0.00	
w× e%	6.97	1.53	- 5.71	- 2.59	13.33	- 0.1	- 0.10	6.19
Pinceti	65.52	15.84	2.50	9.00	3.00	0.0	0.00	
w× e%	7.16	- 6.6	- 2.86	- 3.33	10.00	- 0.1	- 0.10	5.53

Table 4: Discharged energy to ground in each model [Jules]

	Wave		
Arrester model	8/10 μs	4/10 μs	Er%
IEEE	2512	10779	
e%	1.33	- 0.05	0.94
Diaz	2532	12538	
e%	2.14	16.26	11.60
Durbak	2511	11712	
e%	1.29	8.61	6.16
Pinceti	1514	10793	
e%	1.41	0.08	1.00

where, I_{max} and V_{max} are the peak discharge current (in kA) and peak discharge voltage)in kV(respectively and k is considered as 20.8 and 10.4 for 8/20 and 4/10 μs waves, respectively. The results are shown in Table 4.

CONCLUSION

The followings are generally resulted from the tables and simulations:The IEEE 3.4.11 workgroup presented model is the best model from quality and quantity points of view and presents better voltage-current waveforms against fast steep front waves.

The IEEE model encounters with problem in obtaining L1 amount, and A1 and A0 nonlinear resistances regulation if the residual voltage value caused by switching impulse current is not determined properly. The Diaz-Fernandez model is not significantly accurate specially in 4/10 μs impulse wave despite it is well accurate in 8/20 μs waves residual voltages.

The Pinceti model is well accurate in the mentioned time range according to its related algorithm and due to its emphasis on particular front time. Therefore, the Diaz-Fernandez model has a good accuracy just in 8/20 μs wave range.

The Pinceti model does not detect the oscillations of residual voltage wave rear because of capacitor neglecting in the model structure.

REFERENCES

Ahmad, Z., 1994. Effect of Dry Band on Performance of UHVSurge Arrester and Leakage Current Monitoring Using New Developed Model. Proceedings of the 4th International Conference on Properties and Applications of Dielectric Materials, pp: 880-883.

Daniel, W.D., 1985. Zinc-oxide Arrester Model for Fast Surges, EMTP Newsletter, 5(1).

Daniel, W.D., 2001. Surge Arrester Modeling, pp: 728-730.

Diaz, R., F. Fernandez and J. Silva, 2001. Simulation and Test on Surge Arrester in High-Voltage Laboratory, IPST.

Fernandez, F. and R. Diaz, 2001. Metal-Oxide Surge Arrester Model for Fast transient Simulations, IPST.

Penchenat G.,1992. Conaribution a' l'e'tude de dispositifs de protection, Engineering project, Ms. Thesis, Poul Sabatier University, Toulouse, France.

Gupta, T.K., 1990. Application of Zinc Oxide varistors. Am. Ceramic J. Soc., 73: 1817-1840.

IEEE Working Group 3.4.11, 1992. Modeling of metal oxide surge arresters. Power Del. IEEE Trans., 7(1): 302-309.

Kim, I., T. Funabashi, H. Sasaki, T. Hagiwara and M. Kobayashi, 1996. Study of ZNO arrester model for steep front page. IEEE Trans. Power Del., 11(2): 178-185.

Li, H.J., S. Birlasekaran and S.S. Choi, 2002. A parameter identification technique for metal-oxide surge arrester models. Power Eng. Rev. IEEE Trans., 22(4): 79-84.

Pinceti, P. and M. Giannettoni, 1999. A simplified model for zinc oxide surge arresters. IEEE Trans. Power Del., 14(2): 148-154.

Popov, M., L. Van der Sluis and G.C. Poap, 2002. Application of a new surge arrester model in protection studies concerning switching surges. Power Eng. Rev. IEEE, 22(9): 52-53.

PSCAD (EMTDC) default Surge Arrester, 2003. ASEA XAP-A, PSCAD Ruling Book, PSCAD, Version 4.0, pp: 241.

Ravinda, P.S. and T.V.P Singh, 2002. Influence of Pollution on the Performance of Metal Oxide Surge Arresters, Canadian Conference on Electrical and Computer Engineering, pp: 224-229.